39576

P- 24

NASA Technical Memorandum 104124

(NASA-TM-104124) KINEMATICS OF THE SIX-DEGREE-OF-FREEDOM FORCE-REFLECTING KRAFT MASTER (NASA) 24 p CSCL 09B

N91-31?79

Unclas

G3/63 0039576

KINEMATICS OF THE SIX-DEGREE-OF-FREEDOM FORCE-REFLECTING KRAFT MASTER

Robert L. Williams II

July 1991

NASA

National Aeronautics and
Space Administration

Langley Research Center
Hampton, Virginia 23665-5225

KINEMATICS OF THE SIX DEGREE-OF-FREEDOM FORCE-REFLECTING KRAFT MASTER

Dr. Robert L. Williams II
Automation Technology Branch
NASA Langley Research Center

ABSTRACT

This paper presents kinematic equations for a six degree of freedom force-reflecting hand controller. The forward kinematics solution is developed and shown in simplified form. The Jacobian matrix, which uses terms from the forward kinematics solution, is derived. Both of these kinematic solutions require joint angle inputs. A calibration method is presented to determine the hand controller joint angles given the respective potentiometer readings. The kinematic relationship describing the mechanical coupling between the hand controller shoulder and elbow joints is given.

The kinematic equations in this paper may be used in an algorithm to control the hand controller as a telerobotic system component. The purpose of the hand controller is two-fold: 1) Operator commands to the telerobotic system are entered using the hand controller; 2) Contact forces and moments from the task are reflected to the operator via the hand controller.

1 INTRODUCTION

The force-reflecting Kraft Master * is built by Kraft Telerobotics, Inc. It is the master of an undersea master/slave teleoperator system. The "force-reflecting Kraft Master"is referred to hereafter as the "hand controller". The hand controller has right- and left-handed versions for dual arm tasks. The Automation Technology Branch of NASA LaRC uses two such devices for force-reflecting hand controllers in telerobotic systems.

An orthographic view of the right hand controller is shown in Fig. 1. This is an articulated six degree of freedom force-reflecting hand controller. There are six axes whose joint angles are determined from calibration of six potentiometers. For force reflection, torque commands are sent to the first five axes; the wrist roll is not driven.

The hand controller is used to input motion commands into a telerobotic system. The force-reflecting capabilities of the hand controller are used to transmit task forces and moments to the operator. For each communication cycle, five torque commands are written to the hand controller; the controller responds with six potentiometer readings.

The hand controller is used to command position or velocity to a manipulator. Either input mode requires the hand controller forward position transformation. The hand controller Jacobian matrix is used for reflection of task forces to the operator. These kinematic solutions are presented in this paper.

The forward kinematics solution is given first. Following the conventions of Craig (1988), the Denavit-Hartenberg parameters are presented. The homogeneous transformation matrices relating successive coordinate frames are obtained, based on the Denavit-Hartenberg parameters. The forward kinematics solution is the concatenation of these matrices.

* The mention herein of a trademark of a commercial product does not constitute any recommendation for use by the Government.

Rate input commands are generated with the difference of two forward position transformation matrices. A method is presented for determining the difference between two homogeneous transformation matrices. The kinematic relationship of the shoulder and elbow joint coupling is derived. A calibration method is developed to calculate the hand controller joint angles given the potentiometer readings.

The Jacobian matrix of the hand controller with respect to the base frame is presented. It is used for reflection of task forces and moments. The Jacobian matrix also maps hand controller joint velocities into hand controller cartesian velocities.

Examples are given to demonstrate calculations for the potentiometer/joint angle calibration, forward position transformation matrix, and Jacobian matrix.

2 SYMBOLS

$\{m\}$	Cartesian coordinate frame m
$\{B\}$	Base coordinate frame
$\{H\}$	Hand coordinate frame
$\{0\}$	Kinematic base coordinate frame
$\{6\}$	Wrist coordinate frame
$\alpha_{i-1}, a_{i-1}, d_i, \theta_i$	Denavit-Hartenberg parameters
POT_i	Potentiometer readings
θ_i	Joint angle variables
θ_{23}	$\theta_2 + \theta_3$
c_i	$cos\theta_i$
s_i	$sin\theta_i$
$[^n_m T]$	Homogeneous transformation matrix of $\{m\}$ relative to $\{n\}$
$[^n_m R]$	Rotation matrix of $\{m\}$ relative to $\{n\}$
$\{^n P_m\}$	Position vector from origin of $\{n\}$ to $\{m\}$ expressed in $\{n\}$
$L_i, i = 0, \ldots, 5$	Fixed hand controller lengths
K_i	Factored kinematics terms
$RZ,\ RY,\ RX$	Z-Y-X Euler angles
$^k(^j\Omega_i)$	Angular velocity of $\{i\}$ with respect to $\{j\}$ expressed in $\{k\}$
$^m\{\dot{X}\}$	Cartesian rates expressed in $\{m\}$
$\{\dot{\theta}\}$	Joint rates
τ_J	Joint torques
^nF	Manipulator end-effector cartesian forces and moments expressed in $\{n\}$
$^n[J]$	Jacobian matrix expressed in $\{n\}$
$[J_{UL}]$	Upper left partition of the Jacobian matrix
$[J_{LL}]$	Lower left partition of the Jacobian matrix
$[J_{LR}]$	Lower right partition of the Jacobian matrix
θ_{ia}, θ_{ib}	Joint angle endpoints for calibration
POT_{ia}, POT_{ib}	Potentiometer endpoints for calibration

3 FORWARD POSITION KINEMATICS

3.1 Denavit-Hartenberg Parameters

The kinematic diagram for the right hand controller is shown in Fig. 2. All joint angles are zero in Fig. 2. This is not a reachable position due to mechanical limits on the elbow joint. For the coordinate frame definitions in Fig. 2, the Denavit-Hartenberg parameters are given in Table I. The origins of coordinate frames {0}, {1}, and {2} are co-located at point A. The wrist frame origins {4}, {5}, and {6} are co-located at the intersection of the wrist yaw and pitch joints, point B. The origin of {3} is on the X_4, Z_4 plane. The frame $\{H\}$ is located at the hand controller grasp. For both velocity commands and force reflection, {6} is controlled with respect to {0}. Therefore, L_0 and L_5 do not appear in the kinematic equations.

Table I: Denavit-Hartenberg Parameters

i	α_{i-1}	a_{i-1}	d_i	θ_i
1	0	0	0	θ_1
2	90°	0	0	θ_2
3	0	L_1	L_3	θ_3
4	-90°	L_2	L_4	θ_4
5	90°	0	0	$\theta_5 + 90°$
6	90°	0	0	θ_6

Nominal values for the fixed lengths are $L_0 = 203$, $L_1 = 178$, $L_2 = 203$, $L_3 = 133$, $L_4 = 84$, and $L_5 = 114$ (mm).

3.2 Homogeneous Transformation Matrices

The general homogeneous transformation matrix representing the position and orientation of $\{i\}$ with respect to $\{i-1\}$ is given below (Craig, 1988).

$$[{}^{i-1}_{i}T] = \begin{bmatrix} c\theta_i & -s\theta_i & 0 & a_{i-1} \\ s\theta_i c\alpha_{i-1} & c\theta_i c\alpha_{i-1} & -s\alpha_{i-1} & -d_i s\alpha_{i-1} \\ s\theta_i s\alpha_{i-1} & c\theta_i s\alpha_{i-1} & c\alpha_{i-1} & d_i c\alpha_{i-1} \\ 0 & 0 & 0 & 1 \end{bmatrix} \quad (1)$$

The Denavit-Hartenberg parameters of Table I are substituted into Eq. 1 to obtain six homogeneous transformation matrices relating successive coordinate frames. These matrices are reported in Appendix A.

3.3 Forward Position Transformation

The forward kinematics position solution is a mapping from joint space to cartesian space. A homogeneous transformation matrix is used to represent the cartesian position and orientation.

$$[{}^0_6T] = \left[\begin{array}{ccc|c} & [{}^0_6R] & & \{{}^0P_6\} \\ \hline 0 & 0 & 0 & 1 \end{array}\right] \tag{2}$$

The unique forward kinematics solution is a concatenation of the homogeneous transformation matrices.

$$[{}^0_6T] = [{}^0_1T(\theta_1)]\,[{}^1_2T(\theta_2)]\,[{}^2_3T(\theta_3)]\cdots[{}^5_6T(\theta_6)] \tag{3}$$

Substituting the matrices of Appendix A into Eq. 3, the forward kinematics solution is:

$$[{}^0_6T] = \begin{bmatrix} K_2s_6 + K_Ac_6 & -K_As_6 + K_2c_6 & K_C & K_F \\ K_4s_6 + K_Bc_6 & -K_Bs_6 + K_4c_6 & K_D & K_E \\ K_0s_6 + K_6c_6 & -K_6s_6 + K_0c_6 & K_5 & K_9 \\ 0 & 0 & 0 & 1 \end{bmatrix} \tag{4}$$

Common terms K_i are factored out to reduce computation time. These terms, given in Appendix B, also appear in the Jacobian matrix, Eq. 17.

The forward position transformation presented in this section is for the right hand controller. The kinematic diagram for the left hand controller is the same as the right, except the offset L_3 is in the opposite direction. Only one Denavit-Hartenberg parameter from Table I is changed: $d_3 = -L_3$. Therefore, the forward position transformation and Jacobian matrix for the left hand controller are also Eqs. 4 and 17. One change is required: $-L_3$ is substituted for L_3 in terms K_E and K_F of Appendix B.

4 DIFFERENCE OF TWO HOMOGENEOUS TRANSFORMATION MATRICES

One possible hand controller algorithm requires the difference of two $[^0_6T]$ matrices to form velocity commands and return-to-center force errors. The kinematic equations for this operation are presented in this section. The subtraction is not an algebraic subtraction.

$$[^A_{B-C}T] = [^A_BT] - [^A_CT] \tag{5}$$

The translation and orientation decoupling of homogeneous transformation matrices is given in Eq. 2. The difference of two homogeneous transformation matrices is accomplished in two steps, translation and orientation. The translational difference is an algebraic subtraction.

$$\{^AP_{B-C}\} = \{^AP_B\} - \{^AP_C\} \tag{6}$$

With a unity transformation of $\frac{1}{time}$, $\{^AP_{B-C}\}$ is the translational velocity vector error command.

The rotational difference component is more complicated because there is no vector representation for orientation. A relative difference rotation matrix is used, relating the orientation of $\{B\}$ with respect to $\{C\}$.

$$[^C_BR] = [^A_CR]^{-1}\ [^A_BR] = [^A_CR]^T\ [^A_BR] \tag{7}$$

Three orientational difference numbers RZ, RY, RX are extracted from $[^C_BR]$ using the (Z-Y-X) Euler convention (Craig, 1988). The following rotational velocity kinematics transformation is required in order to obtain the angular velocity vector command, expressed in $\{C\}$. Equation 8 is adapted from Appendix II of Kane, et. al. (1983).

$$\begin{aligned} {}^C({}^A\Omega_{B-C})_X &= -\{\dot\theta_Z\}s_Y \quad + \{\dot\theta_X\} \\ {}^C({}^A\Omega_{B-C})_Y &= \quad \{\dot\theta_Z\}c_Y s_X + \{\dot\theta_Y\}c_X \\ {}^C({}^A\Omega_{B-C})_Z &= \quad \{\dot\theta_Z\}c_Y c_X - \{\dot\theta_Y\}s_X \end{aligned} \tag{8}$$

The following assumptions are made for use in Eq. 8.

$$\begin{aligned} \theta_X &= \{\dot\theta_X\} = RX \\ \theta_Y &= \{\dot\theta_Y\} = RY \\ \theta_Z &= \{\dot\theta_Z\} = RZ \end{aligned} \tag{9}$$

Equation 10 transforms the angular velocity vector command into $\{A\}$ coordinates.

$$^{A}({}^{A}\Omega_{D-C}) = [{}^{A}_{C}R]\ {}^{C}({}^{A}\Omega_{D-C}) \tag{10}$$

5 ELBOW JOINT KINEMATICS

The shoulder pitch joint and elbow pitch joint potentiometers and motors are mounted on the link driven by the shoulder yaw joint. The kinematics of the coupling between the shoulder and elbow pitch joints must be determined. This mechanical coupling is a four bar linkage, as shown in Fig. 3.

The four bar linkage coupling does not remove one of the six hand controller degrees of freedom. In Fig. 3, links 1 and 2 rotate independently. If either link 1 or 2 were fixed, or if their motion was not independent, the hand controller would have five degrees of freedom. The following presents the relationships between the second and third potentiometers and joint angles.

The four bar linkage with the Denavit-Hartenberg joint angles is shown in Fig. 4. The second potentiometer measures θ_2, which orients link r_2. The four bar linkage is a parallelogram with $r_1 = r_3 = 32\ mm$ and $r_2 = r_4 = 180\ mm$. The third potentiometer reads the angle which orients link r_1. In the parallelogram four bar linkage, links r_1 and r_3 always have the same orientation angle. The third potentiometer reads $(\theta_2 + \theta_3)$, as shown in Fig. 4.

6 POTENTIOMETER/JOINT ANGLE CALIBRATION

This section details the mapping from potentiometer readings to joint angles for the right and left hand controllers. The potentiometers are linear with nominal range 0 to 4095 counts following A/D conversion. Due to angular limits, none of the potentiometers cover the full range. The calibration of the right and left hand controllers is not identical. The calibration is required to calculate the Denavit-Hartenberg joint angles for the forward position transformation and the Jacobian matrix. The method presented in this section is general, but the potentimeter data in Tables IV and V and the calibration equations, Eqs. 12 and 13, are specific to the hand controllers operated by the Automation Technology Branch of NASA LaRC.

The nominal values for angular limits are given in Table II.

Table II: Nominal Angular Limits

i	θ_{i1}	θ_{i2}
1	$-90°$	$90°$
2	$0°$	$120°$
3	$-135°$	$-35°$
3	$-135°$	$-85°$
4	$-55°$	$55°$
5	$-20°$	$50°$
6	$-45°$	$45°$

There are two ranges given for i = 3 in Table II. The first corresponds to $\theta_2 = 0°$ and the second to $\theta_2 = 120°$. The elbow angle θ_3 has a minimum travel of $50°$ when $\theta_2 = 120°$ and a maximum travel of $100°$ when $\theta_2 = 0°$, due to the mechanical coupling discussed in the previous section.

Table III shows the correspondence among the potentiometers, joint angles, and joint names. The third potentiometer POT_3 directly measures $\theta_2 + \theta_3$. Note that POT_4 and POT_5 are reversed with respect to joint angle index.

Table III: Potentiometer/Joint Angle Correspondence

Potentiometer	Joint Angle	Joint Name
POT_1	θ_1	Shoulder Yaw
POT_2	θ_2	Shoulder Pitch
POT_3	$\theta_2 + \theta_3$	Elbow Pitch
POT_5	θ_4	Wrist Yaw
POT_4	θ_5	Wrist Pitch
POT_6	θ_6	Wrist Roll

The relationship between each potentiometer and the corresponding joint angle is linear. The calibration is accomplished by writing this linear equation between the two angular limits for each joint. The calibration for a general joint is shown in Fig. 5. The two endpoints are ordered pairs of potentiometer count and joint angle, denoted as $(POT_{ia},\ \theta_{ia})$ and $(POT_{ib},\ \theta_{ib})$. The general linear calibration equation is given below, where the variables are $(POT_i,\ \theta_i)$.

$$\theta_i = \theta_{ia} + \left(\frac{\theta_{ib} - \theta_{ia}}{POT_{ib} - POT_{ia}}\right)(POT_i - POT_{ia}) \tag{11}$$

Table IV gives the measured values for each joint of the right hand controller and Table V the left. For the elbow joint there are two different limit ranges, depending on the value of θ_2. The two extreme endpoints are used for the POT_3 equation. The positive joint angle convention does not necessarily match a positive change in potentiometer counts.

Table IV: Calibration Data for Right Hand Controller

Potentiometer Index	POT_{ia}	POT_{ib}	θ_{ia}	θ_{ib}
1	157	4014	90°	−90°
2	751	3328	0°	120°
3	248	3863	35°	−135°
5	500	2930	55°	−55°
4	1126	2766	−20°	50°
6	1395	2656	45°	−45°

Table V: Calibration Data for Left Hand Controller

Potentiometer Index	POT_{ia}	POT_{ib}	θ_{ia}	θ_{ib}
1	119	3983	90°	-90°
2	777	3354	0°	120°
3	240	3859	35°	-135°
5	808	3280	55°	-55°
4	1228	2856	-20°	50°
6	1402	2634	45°	-45°

The calibration equations are obtained by evaluating Eq. 11 with the data of Tables IV and V. The results are expressed in radians. Equation 12 is for the right hand controller and Eq. 13 is for the left.

$$
\begin{aligned}
\theta_1 &= 1.699 - 8.145\times10^{-4}POT_1 \\
\theta_2 &= -0.610 + 8.127\times10^{-4}POT_2 \\
\theta_2 + \theta_3 &= 0.814 - 8.208\times10^{-4}POT_3 \\
\theta_4 &= 1.355 - 7.901\times10^{-4}POT_5 \\
\theta_5 &= -1.188 + 7.450\times10^{-4}POT_4 \\
\theta_6 &= 2.523 - 12.457\times10^{-4}POT_6
\end{aligned} \tag{12}
$$

$$
\begin{aligned}
\theta_1 &= 1.668 - 8.130\times10^{-4}POT_1 \\
\theta_2 &= -0.631 + 8.127\times10^{-4}POT_2 \\
\theta_2 + \theta_3 &= 0.808 - 8.198\times10^{-4}POT_3 \\
\theta_4 &= 1.587 - 7.766\times10^{-4}POT_5 \\
\theta_5 &= -1.271 + 7.504\times10^{-4}POT_4 \\
\theta_6 &= 2.573 - 12.750\times10^{-4}POT_6
\end{aligned} \tag{13}
$$

Due to the sensitivity of the potentiometers and the uncertainty in joint angle measurements, an improved calibration method would read several (POT_i, θ_i) combinations for each joint and then obtain a linear least-squares fit. Upon implementation, the results of Eqs. 12 and 13 were judged to be sufficiently accurate, and thus the improved method was not pursued.

From inspection of Eqs. 4 and 17 and Appendix B, neither the forward position transformation nor the Jacobian matrix require θ_3 explicitly. The sum $\theta_2 + \theta_3$ is required and available directly from the calibration equation for POT_3.

7 JACOBIAN MATRIX

The Jacobian matrix is a linear operator which maps joint space velocities to cartesian velocities. The Jacobian matrix order is six by six for the hand controller.

$$^{m}\{\dot{X}\} = {}^{m}[J]\{\dot{\theta}\} \tag{14}$$

The transpose of the Jacobian matrix transforms cartesian forces and moments to joint torques.

$$\tau_J = {}^{m}[J]^T \;\; {}^{m}\{F\} \tag{15}$$

The vector of cartesian forces and moments at the manipulator end-effector is $^{m}\{F\}$. Hand controller joint torques τ_J reflect $^{m}\{F\}$ to the operator at the hand controller wrist. The Jacobian matrix and the cartesian force/moment vector are expressed in frame $\{m\}$. The Jacobian matrix with respect to $\{0\}$ requires fewer calculations than with respect to $\{6\}$ and so $m = 0$ is used.

$$^{0}[J] = \begin{bmatrix} J_{11} & J_{12} & J_{13} & 0 & 0 & 0 \\ J_{21} & J_{22} & J_{23} & 0 & 0 & 0 \\ 0 & J_{32} & J_{33} & 0 & 0 & 0 \\ 0 & J_{42} & J_{43} & J_{44} & J_{45} & J_{46} \\ 0 & J_{52} & J_{53} & J_{54} & J_{55} & J_{56} \\ 1 & 0 & 0 & J_{64} & J_{65} & J_{66} \end{bmatrix} \tag{16}$$

The upper right three by three submatrix of the Jacobian is the zero matrix because the wrist frames $\{4\}$ through $\{6\}$ share a common origin.

$$^{0}[J] = \begin{bmatrix} [J_{UL}] & | & [0] \\ --- & | & --- \\ [J_{LL}] & | & [J_{LR}] \end{bmatrix} \tag{17}$$

$$[J_{UL}] = \begin{bmatrix} -K_E & -K_9 c_1 & -K_7 c_1 \\ K_F & -K_9 s_1 & -K_7 s_1 \\ 0 & K_{10} & K_8 \end{bmatrix} \tag{17a}$$

$$[J_{LL}] = \begin{bmatrix} 0 & s_1 & s_1 \\ 0 & -c_1 & -c_1 \\ 1 & 0 & 0 \end{bmatrix} \tag{17b}$$

$$[J_{LR}] = \begin{bmatrix} -c_1 s_{23} & K_2 & K_C \\ -s_1 s_{23} & K_4 & K_D \\ c_{23} & K_0 & K_5 \end{bmatrix} \tag{17c}$$

The kinematic terms for the Jacobian matrix, also used in the forward position transformation (Eq. 4), are given in Appendix B.

8 EXAMPLES

Two examples of the potentiometer/joint angle calibration, forward position transformation matrix and the Jacobian matrix for the right hand controller are given in this section. The input is the vector of potentiometer counts, $POT_1, \ldots, POT_6$. Output is $\{\theta\}$, $[^0_6T]$, and $^0[J]$ using Eqs. 12, 4, and 17, respectively. The examples use the nominal values for L_1, L_2, L_3, and L_4 given in Section 3.1.

The position of Example 1 is shown in Fig. 1. This is a good default initial position.

1) $\{POT\} = \{2086, 2683, 992, 1595, 1715, 2025\}^T$

$$\{\theta\} = \{0.0, 90.0, -90.0, 0.0, 0.0, 0.0\}^T$$

$$[^0_6T] = \begin{bmatrix} 0.000 & 0.000 & 1.000 & 203.000 \\ 0.000 & -1.000 & 0.000 & -133.000 \\ 1.000 & 0.000 & 0.000 & 262.000 \\ 0 & 0 & 0 & 1 \end{bmatrix}$$

$$^0[J] = \begin{bmatrix} 133.000 & -262.000 & -84.000 & 0.000 & 0.000 & 0.000 \\ 203.000 & 0.000 & 0.000 & 0.000 & 0.000 & 0.000 \\ 0.000 & 203.000 & 203.000 & 0.000 & 0.000 & 0.000 \\ 0.000 & 0.000 & 0.000 & 0.000 & 0.000 & 1.000 \\ 0.000 & -1.000 & -1.000 & 0.000 & -1.000 & 0.000 \\ 1.000 & 0.000 & 0.000 & 1.000 & 0.000 & 0.000 \end{bmatrix}$$

Example 2 is a general position.

2) $\{POT\} = \{2622, 1610, 2268, 1829, 2488, 1745\}^T$

$$\{\theta\} = \{-25.0, 40.0, -100.0, -35.0, 10.0, 20.0\}^T$$

$$[^0_6T] = \begin{bmatrix} 0.498 & -0.826 & 0.263 & 225.293 \\ -0.438 & -0.502 & -0.746 & -251.805 \\ 0.748 & 0.256 & -0.612 & -19.387 \\ 0 & 0 & 0 & 1 \end{bmatrix}$$

$$^0[J] = \begin{bmatrix} 251.805 & 17.571 & 121.267 & 0.000 & 0.000 & 0.000 \\ 225.293 & -8.193 & -56.548 & 0.000 & 0.000 & 0.000 \\ 0.000 & 310.602 & 174.246 & 0.000 & 0.000 & 0.000 \\ 0.000 & -0.423 & -0.423 & 0.785 & -0.606 & 0.263 \\ 0.000 & -0.906 & -0.906 & -0.366 & -0.621 & -0.746 \\ 1.000 & 0.000 & 0.000 & 0.500 & 0.497 & -0.612 \end{bmatrix}$$

9 CONCLUSION

This paper presents kinematic equations for control of a six degree of freedom force-reflecting hand controller. The hand controller is used for commanding motion and reflecting forces in a telerobotic system. The forward kinematics solution and Jacobian matrix are derived for control of the hand controller wrist with respect to the base. A method is given for finding the difference between two homogeneous transformation matrices to form velocity commands and return-to-center force for the hand controller. The mechanical coupling between the shoulder and elbow pitch joints is investigated. A calibration method is presented to calculate the hand controller joint angles given the potentiometer readings. Numerical examples are given for the equations. This paper gives the kinematic equations required for control of this force-reflecting hand controller.

10 REFERENCES

Craig, J.J., **Introduction to Robotics: Mechanics and Control**, Addison Wesley Publishing Co., Reading, MA, 1988.

Kane, T. R., Likins, P. W., and Levinson, D. A., **Spacecraft Dynamics** , McGraw-Hill Book Co., New York, 1983.

Kraft TeleRobotics, Inc., "*Force Feedback GRIPS Manipulator, KMC 9100F Electronics System Manual*", 11667 W. 90th St., Overland Park, KS 66214, Telephone: (913) 894-9022.

Kraft TeleRobotics, Inc., "*KMC 9100S Interface, 700-9049-00, System Manual*", 11667 W. 90th St., Overland Park, KS 66214, Telephone: (913) 894-9022.

APPENDIX A: HOMOGENEOUS TRANSFORMATION MATRICES

Six homogeneous transformation matrices are given in this appendix, relating frame $\{i\}$ to $\{i-1\}$ for the hand controller, where $i = 1, 2, \ldots, 6$. These matrices are obtained by substituting the Denavit-Hartenberg parameters of Table I into Eq. 1.

$$[{}^0_1T] = \begin{bmatrix} c_1 & -s_1 & 0 & 0 \\ s_1 & c_1 & 0 & 0 \\ 0 & 0 & 1 & 0 \\ 0 & 0 & 0 & 1 \end{bmatrix}$$

$$[{}^1_2T] = \begin{bmatrix} c_2 & -s_2 & 0 & 0 \\ 0 & 0 & -1 & 0 \\ s_2 & c_2 & 0 & 0 \\ 0 & 0 & 0 & 1 \end{bmatrix}$$

$$[{}^2_3T] = \begin{bmatrix} c_3 & -s_3 & 0 & L_1 \\ s_3 & c_3 & 0 & 0 \\ 0 & 0 & 1 & L_3 \\ 0 & 0 & 0 & 1 \end{bmatrix}$$

$$[{}^3_4T] = \begin{bmatrix} c_4 & -s_4 & 0 & L_2 \\ 0 & 0 & 1 & L_4 \\ -s_4 & -c_4 & 0 & 0 \\ 0 & 0 & 0 & 1 \end{bmatrix}$$

$$[{}^4_5T] = \begin{bmatrix} -s_5 & -c_5 & 0 & 0 \\ 0 & 0 & -1 & 0 \\ c_5 & -s_5 & 0 & 0 \\ 0 & 0 & 0 & 1 \end{bmatrix}$$

$$[{}^5_6T] = \begin{bmatrix} c_6 & -s_6 & 0 & 0 \\ 0 & 0 & -1 & 0 \\ s_6 & c_6 & 0 & 0 \\ 0 & 0 & 0 & 1 \end{bmatrix}$$

APPENDIX B: FACTORED KINEMATICS TERMS

The common kinematic terms for the forward position transformation, Eq. 4, and the Jacobian matrix, Eq. 17, are given below.

$$
\begin{aligned}
K_0 &= s_{23}s_4 \\
K_i &= c_1c_{23} \\
K_j &= s_1c_{23} \\
K_m &= s_{23}c_5 \\
K_n &= s_{23}s_5 \\
K_1 &= s_1s_4 - K_ic_4 \\
K_2 &= s_1c_4 + K_is_4 \\
K_3 &= -c_1s_4 - K_jc_4 \\
K_4 &= -c_1c_4 + K_js_4 \\
K_5 &= c_{23}s_5 + K_mc_4 \\
K_6 &= c_{23}c_5 - K_nc_4 \\
K_7 &= L_2s_{23} + L_4c_{23} \\
K_8 &= L_2c_{23} - L_4s_{23} \\
K_9 &= K_7 + L_1s_2 \\
K_{10} &= K_8 + L_1c_2 \\
K_A &= K_1s_5 - K_mc_1 \\
K_B &= K_3s_5 - K_ms_1 \\
K_C &= -K_1c_5 - K_nc_1 \\
K_D &= -K_3c_5 - K_ns_1 \\
K_E &= K_{10}s_1 - L_3c_1 \\
K_F &= K_{10}c_1 + L_3s_1
\end{aligned}
$$

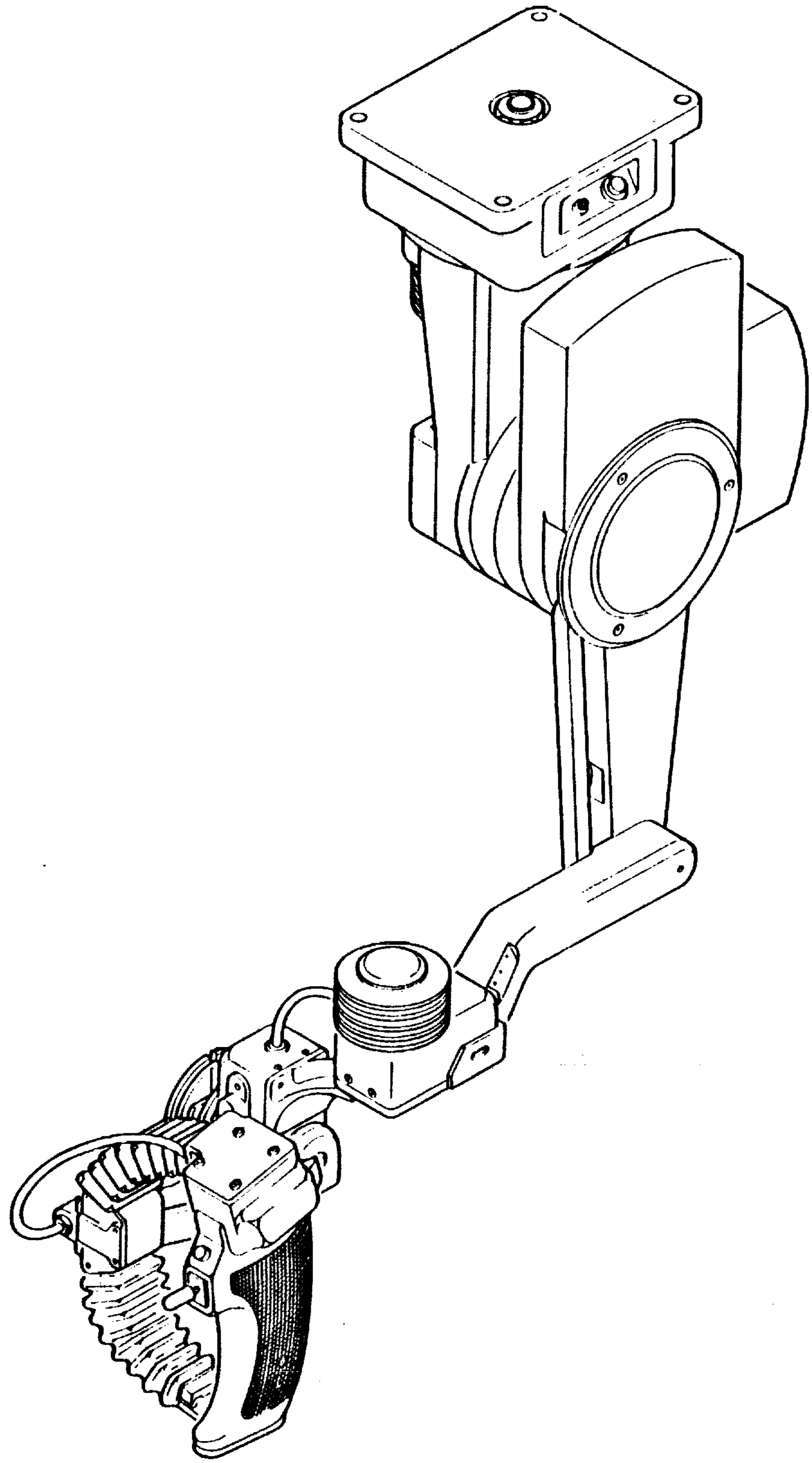

Figure 1
Right Kraft Master
Orthographic View

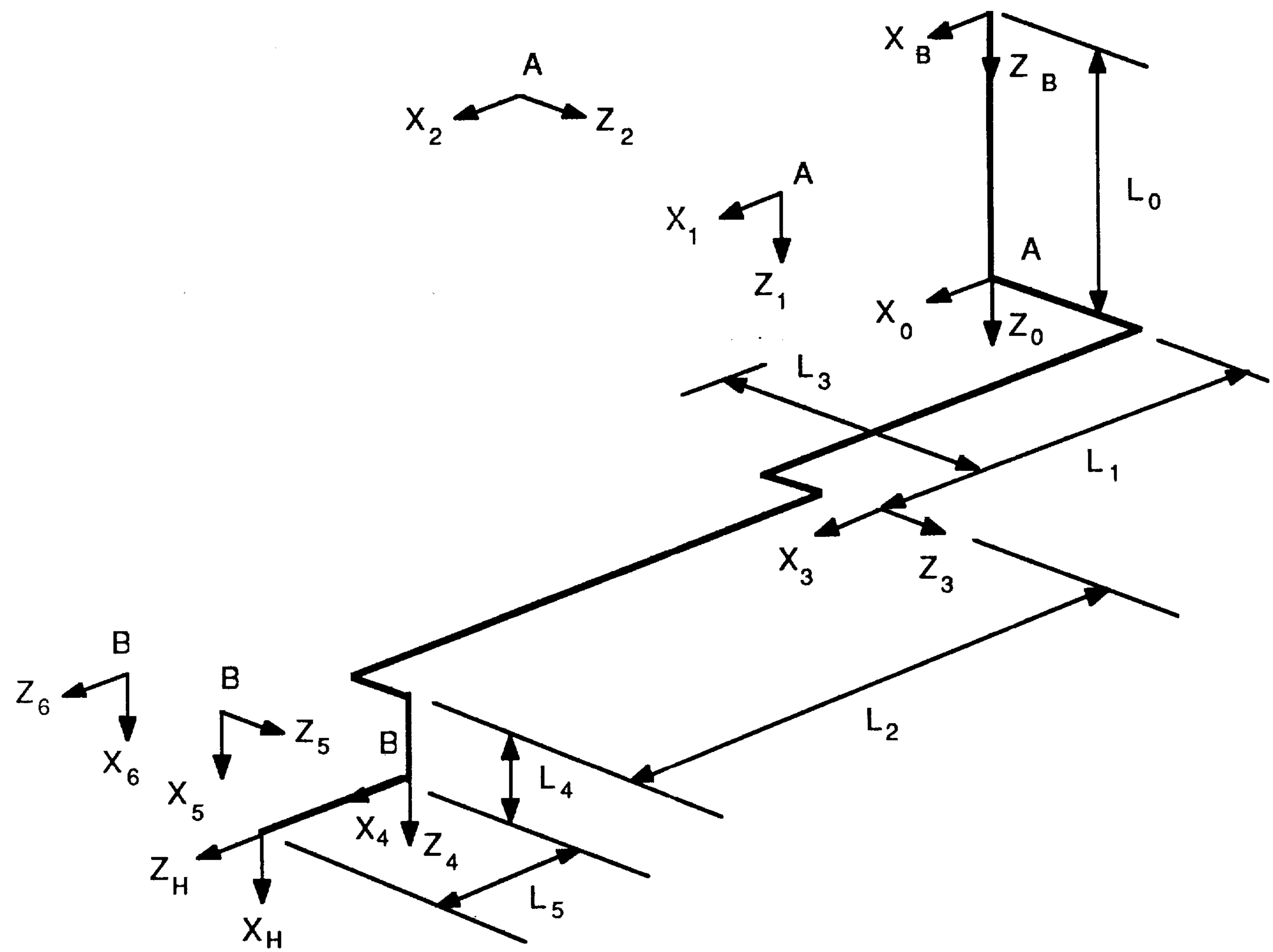

Figure 2
Right Kraft Master
Kinematic Diagram

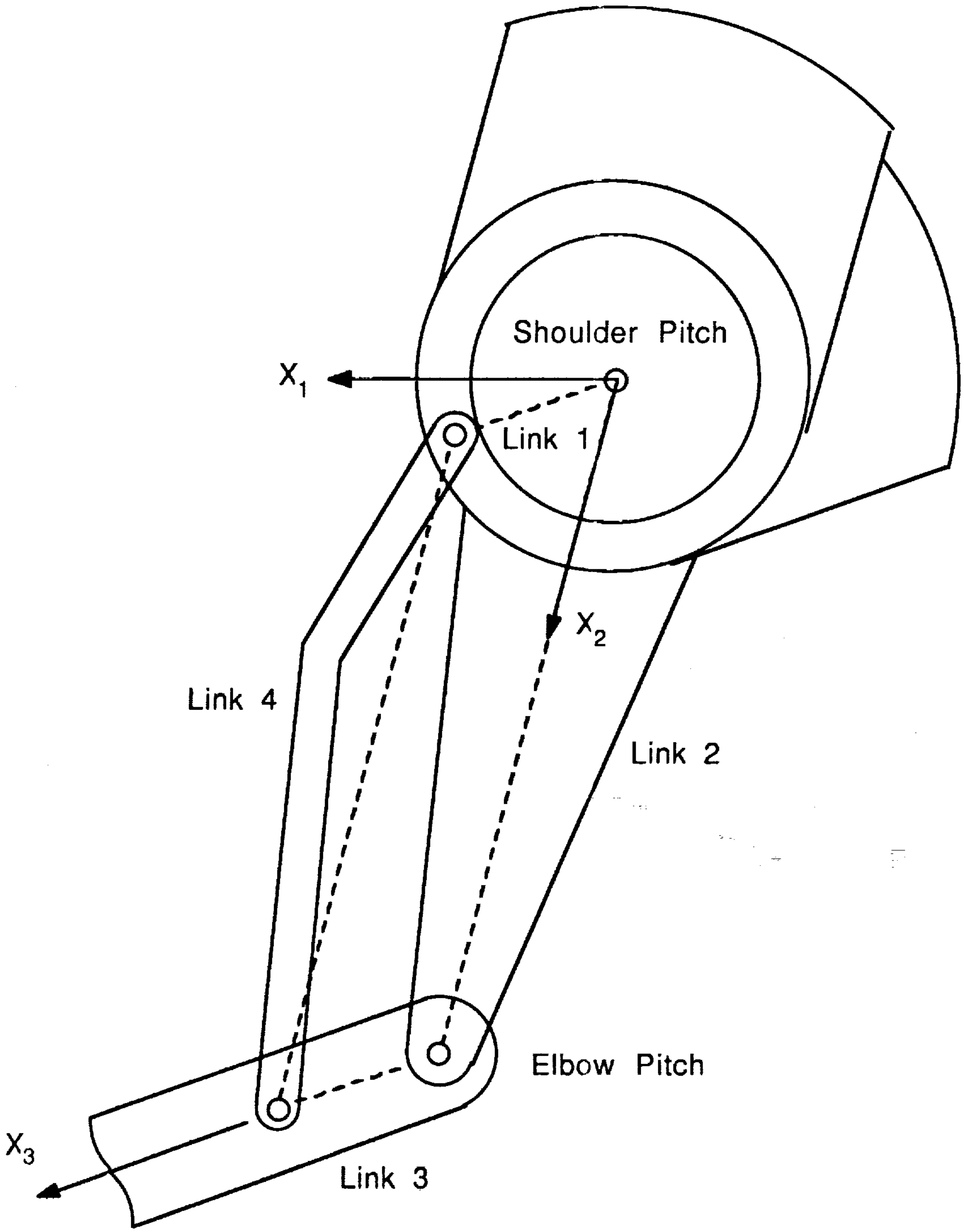

Figure 3
Mechanical Coupling of the
Shoulder/Elbow Pitch Joints

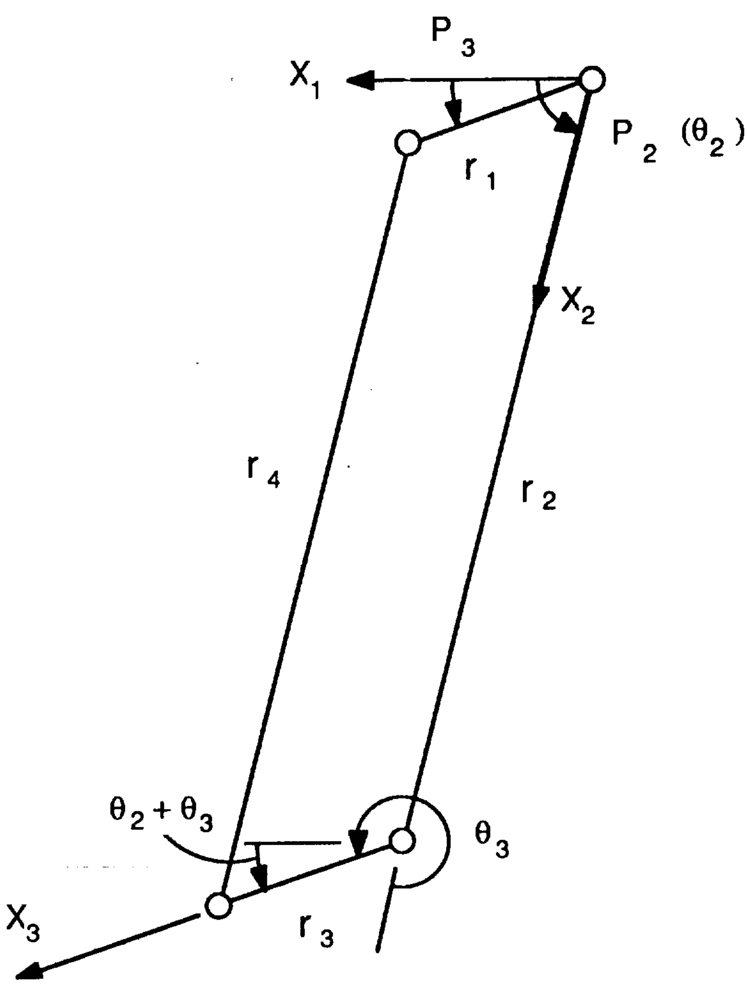

Figure 4
Four-Bar Linkage Kinematic Diagram
with Denavit-Hartenberg Angles

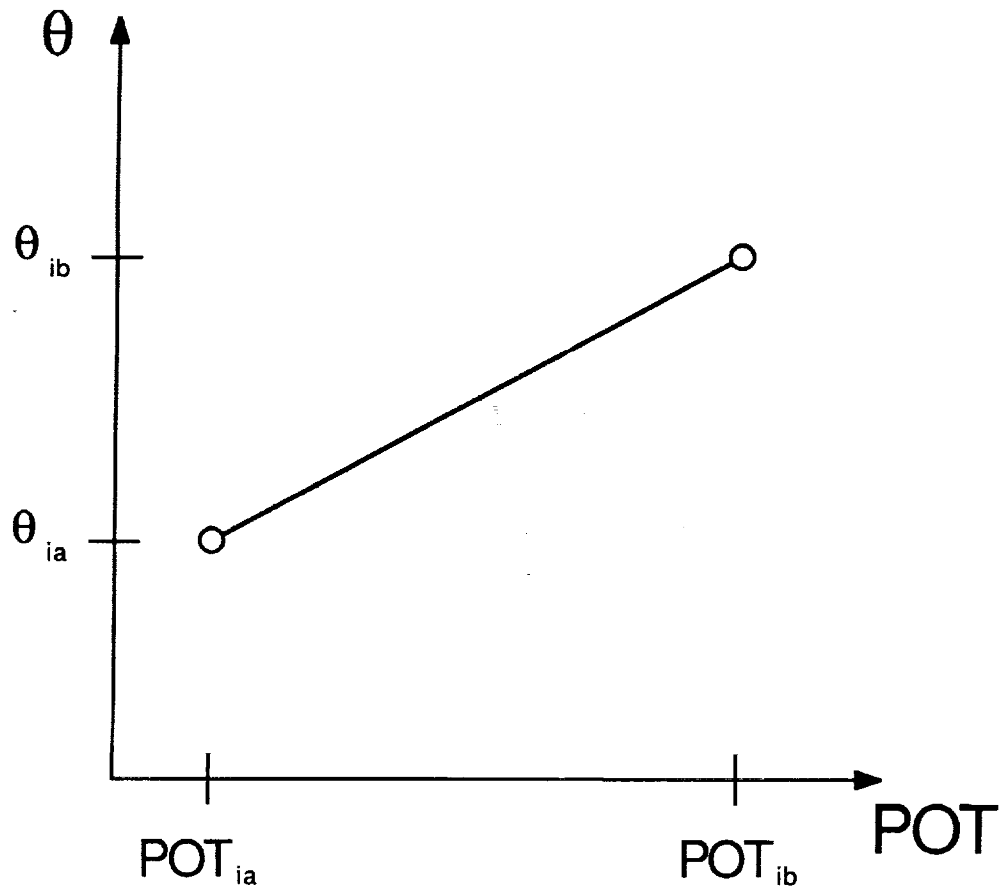

Figure 5
Two-Point Linear Calibration from
Potentiometer to Joint Angle

Report Documentation Page

National Aeronautics and Space Administration

1. Report No.	NASA TM-104124
2. Government Accession No.	
3. Recipient's Catalog No.	
4. Title and Subtitle	Kinematics of the Six-Degree-of-Freedom Force-Reflecting Kraft Master
5. Report Date	July 1991
6. Performing Organization Code	
7. Author(s)	Robert L. Williams II
8. Performing Organization Report No.	
9. Performing Organization Name and Address	NASA Langley Research Center Hampton, VA 23665-5225
10. Work Unit No.	590-11-22-01
11. Contract or Grant No.	
12. Sponsoring Agency Name and Address	National Aeronautics and Space Administration Washington, DC 20546-0001
13. Type of Report and Period Covered	Technical Memorandum
14. Sponsoring Agency Code	
15. Supplementary Notes	

16. Abstract

This paper presents kinematic equations for the six-degree-of-freedom force-reflecting Kraft Master. The forward kinematics solution is presented in simplified form. The Jacobian matrix is presented, which uses terms from the forward kinematics solution. Both of these kinematic solutions require joint angle inputs. A calibration method is presented to determine the Kraft Master joint angles given the respective potentiometer readings. The kinematic relationship describing the mechanical coupling between the Kraft Master shoulder and elbow joints is derived.

The kinematic equations in this paper may be used in an algorithm to control the Kraft Master as a telerobotic system component. The purpose of the Kraft Master is two-fold: (1) Operator commands to the telerobotic system are entered using the Kraft Master; (2) Contact forces and moments from the task are reflected to the operator via the Kraft Master.

17. Key Words (Suggested by Author(s))	Hand Controller Force Reflection Telerobotics Kinematics Master-Slave Manipulator
18. Distribution Statement	Unclassified - Unlimited Star Category 63
19. Security Classif. (of this report)	Unclassified
20. Security Classif. (of this page)	Unclassified
21. No. of pages	23
22. Price	A03